World Electric Vehicle Journal

MDPI

Article

Design Analysis of High-Power Level 4 Smart Charging Infrastructure Using Next-Generation Power Devices for EVs and Heavy Duty EVs

Tehseen Ilahi [1,2,*], Tahir Izhar [1], Muhammad Zahid [2], Akhtar Rasool [3,*], Kelebaone Tsamaase [3], Tausif Zahid [2] and Ehtisham Muhammad Khan [2]

[1] Department of Electrical Engineering, University of Engineering and Technology, Lahore 54890, Pakistan; tizhar@gmail.com
[2] Department of Electrical Engineering, Riphah International University, Lahore 54000, Pakistan; muhammad.zahid@riphah.edu.pk (M.Z.); tausif.zahid@riphah.edu.pk (T.Z.); ehtisham.muhammad@riphah.edu.pk (E.M.K.)
[3] Department of Electrical Engineering, University of Botswana, Gaborone UB0061, Botswana; tsamaasek@ub.ac.bw
* Correspondence: tehseen.ilahi@riphah.edu.pk (T.I.); akhtar@sabanciuniv.edu (A.R.)

Abstract: Trending electric vehicles with different battery technologies need universally compatible and fast chargers. Present semiconductor technology is not suitable for designing high-power-rating converters. The increasing demand for high-capacity electric vehicle chargers requires efficient and optimum advanced material technology. This research presents next-generation material-based smart ultra-fast electric vehicle charging infrastructure for upcoming high-capacity EV batteries. The designed level 4 charger will be helpful for charging future heavy-duty electric vehicles with battery voltages of up to 2000 V. The designed infrastructure will be helpful for charging both EVs and heavy-duty electric trucks with a wide range of power levels. Wireless sensor-based smart systems monitor and control the overall charging infrastructure. The detailed design analysis of the proposed charger using the Simscape physical modeling tool is discussed using mathematical equations.

Keywords: ultra-fast charger; heavy electric vehicles charging; next-generation power devices; bidirectional converters; MATLAB Simscape modeling

Citation: Ilahi, T.; Izhar, T.; Zahid, M.; Rasool, A.; Tsamaase, K.; Zahid, T.; Khan, E.M. Design Analysis of High-Power Level 4 Smart Charging Infrastructure Using Next-Generation Power Devices for EVs and Heavy Duty EVs. *World Electr. Veh. J.* **2024**, *15*, 66. https://doi.org/10.3390/wevj15020066

Academic Editors: Gregorio Cappuccino and Giovanni Pede

Received: 31 December 2023
Revised: 25 January 2024
Accepted: 5 February 2024
Published: 14 February 2024

1. Introduction

Global warming and energy are the main concerns of the modern day. Natural-resource-based transportation systems are major causes of global emission problems [1,2]. Green and efficient transportation electrical vehicle (EV) mobility is the compulsion of the 21st century [3]. Technology is driven by energy, whether a small-scale electronic gadget, industry machinery, or a warship. Moreover, the emissions of CO_2 from internal combustion engine vehicles affect the environment by increasing the air pollution [4,5]. The necessity of energy resources due to the depletion of fossil fuel reserves and transitioning to eco-friendly technology led to the development of electric vehicles (EVs). The demand for electric vehicles is increasing and is expected to achieve more global recognition in the coming years [6]. There are many benefits of EVs, such as zero carbon emissions, non-reliance on fossil fuels, eco-friendliness, and helping power be fed back to the grid. However, there are negative aspects of EVs, which include charging of EV batteries; long charging times; fear of not being able to drive the desired distance with a charged battery; the cost of charging, especially fast charging at peak hours specifically; long charging queues at charging stations; expensive charging infrastructure; and the fact that bidirectional charging from the grid may affect the power quality of the grid and degrade EV batteries.

In the rapidly growing realm of electric vehicle technology, the demand for high-power ultra-fast chargers has reached unprecedented levels. The sales trends of electric vehicles (EVs), battery electric vehicles (BEVs), and plug-in hybrid electric vehicles (PHEVs) have continuously climbed for the last few years [7]. The power trains that are best for pollution reduction are EVs or BEVs, since they generate zero emissions during usage [8]. In world efforts to control the global warming effect, it will become mandatory to provide sustainable infrastructure for EV charging, both domestically and commercially across the globe.

The charging infrastructure varies for different types of vehicles based upon the weight of the vehicles [9]. This is due to the electric power requirements of these vehicles and the distances they travel. Electric vehicles are divided into three different types based upon their use and weight, i.e., light-duty vehicles, medium-duty vehicles, and heavy-duty vehicles (HDEVs) or heavy electric vehicles (HEVs). They can be charged using either AC or DC charging systems. The first strategy is charging from a charging station using a plug-in cable, i.e., conductive charging. The second method is charging through induction, i.e., inductive charging. The third is battery swapping, i.e., changing the empty battery with an already charged battery. The charging method most commonly in use is charging directly through cables, i.e., conductive charging [10].

To achieve the goal of fast-charging, high-power-rating charging devices with fast switching speeds are required. Fast switching and high ratings can be achieved by using advanced material power devices. Power electronic converters have great importance in many power applications, as they control the flow of electric power efficiently. Silicon-based semiconductor devices have been used in power electronics for a long time. Due to their low electrical characteristics like voltage level, efficiency, capacity, and size, the use of semiconductor devices has become limited in high-power and fast-switching applications. To overcome the limitations of silicon devices, scientists developed wideband gap (WBG) and ultrawideband gap (UWBG) material switching devices, which have high electrical characteristics. The comparison of different material devices is summarized in Table 1.

Table 1. Characteristic comparisons of a few materials [11,12].

Sr	Type of Material	Band Gap (eV)	Density (g/cm^3)	Critical Field (MV/cm)	Peak Rated Voltages	Peak Rated Current
1	Si	1.1	2.3	0.3	1 kV	≈100 A
2	SiC (WBG)	3.3	6.12	3.1	10 kV	≈1000 A
3	GaN (WBG)	3.5	3.2	4.9	10 kV	≈1000 A
4	AIN/AlGaN (UWBG)	~6	3.3	15.4	100 kV	≈10,000 A
5	B-Ga_2O_3 (UWBG)	4.9	6.4	10.3	100 kV	≈10,000 A

Generally, there are two types of charging system based upon infrastructure. They are known as on-board charging systems and off-board charging systems. In an on-board charging system, the charge converter and other circuitry is placed inside the EV battery storage system. In an off-board charging system, the charge converter and other circuitry are placed outside the EV while the battery storage system is inside the EV. The charging systems, both DC and AC, are divided into three levels based upon their power level. The level 1 charging system is residential charging. It is operated on a single-phase charging system with a power level of 1.4 kW or 1.9 kW. Level 2 can either be connected to a single-phase or three-phase charging system. It can operate on 208–240 V charging systems with ratings of 80 A (max) and power levels of 4 kW, 8 kW, and 19.2 kW at charging currents of 17 A, 32 A, and 80 A, respectively. Level 3, also known as DC fast charging or rapid charging, can operate on 208–600 V charging systems (AC or DC) with power levels of 50 kW and 100 kW. Research is being carried out on further increasing the charging speed to 400 kW, which is known as extreme or ultra-fast charging [13].

Typically, a fast charger uses three-phase (440–480 V) power lines connected to a step-down transformer. The latest ABB, Tesla, and NEX2 EVs have introduced DC fast chargers with capacities above 100 kW (350 kW max) [14]. A few researchers have introduced medium-voltage (MV), directly connected EV chargers using the latest material semiconductor devices [14]. These direct grid tie chargers use silicon carbide (SiC)-based rectifiers without proper power factor correction and DC bus voltage control. Currently, the available latest technology EV charger is designed for 400 V or 800 V battery packs of EVs. The next generation quickly replaces the voltage level up to 1200 V or 1400 V [15]. A higher voltage level decreases the current level, hence, conductor size, losses, and power devices' current handling limit are reduced. The renewable integrated charging station can abate the charging cost and reduce environmental pollution. The smart distribution system also decreases the power dip and high-cost problem, and it also improves the power quality [16,17]. Solid-state transformers (SST) are suitable for medium voltage (1 kV to 35 kV) conversion of AC/DC power with a medium frequency range (300 Hz to 3000 kHz) as compared to traditional transformers. The SST-based system also improves the power quality of the grid and reduces the overall weight and volume. These topologies are most recommended for DC grid systems for providing better regulation and power quality [18,19].

The latest WBG technology power devices are designed for 1200 V level and can handle a few amperes at high frequencies under safe area operation. For high breakdown voltage and current density, next-generation UWBG technology-based power devices are highly focused on in research [20]. UWBG materials are better suited for attaining power devices in the near range of 10–15 kV, with a breakdown voltage of up to 5 kV. They can handle switching frequency of GHz, which will help reduce filter size. It will reduce the number of power devices due to high breakdown voltage during reverse bias and huge power handling. These materials offer low-stat resistance (R_{ds}) and current density of 3 kA/cm^2 [20]. Future advanced power electronic material devices can be most helpful in designing high-power converters. The current available EV chargers fail to provide proper authentication, real-time parameter monitoring systems, diagnostics alerts, maintenance alerts, etc. Wireless sensor networks (WSN) and Internet of Things (IoT)-based smart systems with data cloud integration are needed in this modern era [21].

The research proposed a high-power (up to 1 MW) fast EV charging infrastructure for existing and upcoming high-density EV battery technology. All the commercially available EV chargers are under 400 kW and are not suitable to charge battery voltage above 1000 V [22]. Present silicon-based semiconductor devices are not suitable for designing high-power converters for EV charging applications. The research proposed next-generation semiconductor-material (ultra-wideband gap)-device-based power converters designed for EV charging applications. The technology of these devices has remarkable potential that will extend the power levels up to the next level. The future electric buses have a battery voltage level of more than 1000 V for high-power handling with minimum charging time. The designed charger will support the high charging voltage level of both EVs and electric buses up to 2000 V DC.

Research Contributions and Paper Structure

In this research, electric vehicle chargers designed by using AC–DC and DC–DC power converters based on next-generation power devices (UWBG) were designed. The paper highlights the important aspects of developing a reliable and efficient electric vehicle charging system for electric vehicles (EV) and heavy electric vehicles (HEV). The research proposed novel advanced material-based smart ultra-fast electric vehicle charging infrastructure for high-capacity EV batteries. The article introduced a new level 4 charging infrastructure with a power capacity of 1 MW for EVs and electric buses (E-buses) having smart features.

The designed level 4 charger also supports upcoming heavy electric vehicles with battery voltages of 1200–2000 V and will charge them within a few minutes. UWBG materials are the future of next-generation high-power devices. Using these materials, high power converters can be designed using a smaller number of devices, hence, reducing the size, weight, and control complexity of the system. A WSN-based IoT system monitors and controls the overall charging infrastructure. The research presented the complete design procedure and Simscape (MATLAB 2019, MathWorks, Inc. Natick, MA, USA) physical simulation analysis of the proposed system.

In Section 2, the detailed design procedure of the proposed mega power smart fast-charging infrastructure is discussed. Gallium trioxide (Ga_2O_3)-based power device SPICE model is used to model high-power converters. Section 3 discussed the model calculation of converters, high-frequency transformers, and filter values. The physical modeling of the proposed charging infrastructure in MATLAB Simscape environment is presented in Section 4. In Section 5, the simulation results are analyzed. The research discussion and conclusion are summarized in Sections 6 and 7, respectively.

2. Proposed Mega Power Smart Fast-Charging Infrastructure

The proposed novel smart ultra-fast mega EV charging station is the next level 4 innovation in charging technology infrastructure that will power both current and future electric vehicle technologies with IoT-enabled features. The charger will be able to charge EV or heavy electric vehicles (HEV) batteries up to 2 kV voltage level with a power capacity of 1 MW. The active dual-control (DC bus and charging voltage) with unity power factor controls the transfer of energy from AC bus to the EV battery in the most effective way and provides a wide range of charging levels for EVs like Tesla, Mercedes, Nissan, Ford, etc. The proposed charging station, with its quick charging times, cutting-edge smart technologies, and scalability to accommodate the variety in electric vehicles, represents a ground-breaking advancement in the infrastructure for electric vehicles. These stations serve as the foundation of a cleaner, more environmentally friendly transportation system, as the automotive industry makes a massive move towards electrification.

The charging level 4 mega power infrastructure is designed using ultra-wideband-material-based power devices. In this research, the gallium trioxide (Ga_2O_3) material of the UWBG category is selected due to easy availability, cost-effectiveness, and technical maturity [23,24]. UWBG materials have better figure of merit (FOM) as compared to silicon and carbide technology [25,26]. The SPICE model of Ga_2O_3 Power MOSFET is used to model the proposed infrastructure [27]. It consists of interleaved bi-directional DC chargers' modules to charge the EV battery from the DC bus that is connected to the AC bus via an AC/DC converter. The three DC/DC converter modules operate in parallel with the same switching frequency known as interleaved techniques to handle high charging current. The bi-directional power converter can control power in both directions i.e., grid to a vehicle (G2V) and vehicle to grid (V2G). The AC bus is connected to the traditional AC grid and renewable energy systems to overcome the grid burden, enable cost-effectiveness, and, most importantly, to mitigate environmental issues [28]. The energy-storing unit consists of power storing devices, mainly high-density batteries and ultra-fast supercapacitors. That will increase voltage levels, improve power availability, and enhance system reliability. The complete proposed infrastructure is shown in Figure 1.

The smart IoT-enabled system provides various features to electric vehicle charging systems [29,30]. This is achieved by an effective communication system with an advanced sensing network also known as a wireless sensor network (WSN) with controllers. The charging module continuously observes the charging parameters and battery information by using WSN. The information and reading are sent to the central control system, service provider, user, and data cloud. The cloud data information will be further helpful to improve system performance, charging behavior, battery degradation alert, fault diagnostics, etc., by IoT application [31,32]. Other sensors are linked with control systems wirelessly to monitor and control the power flow of AC and DC buses.

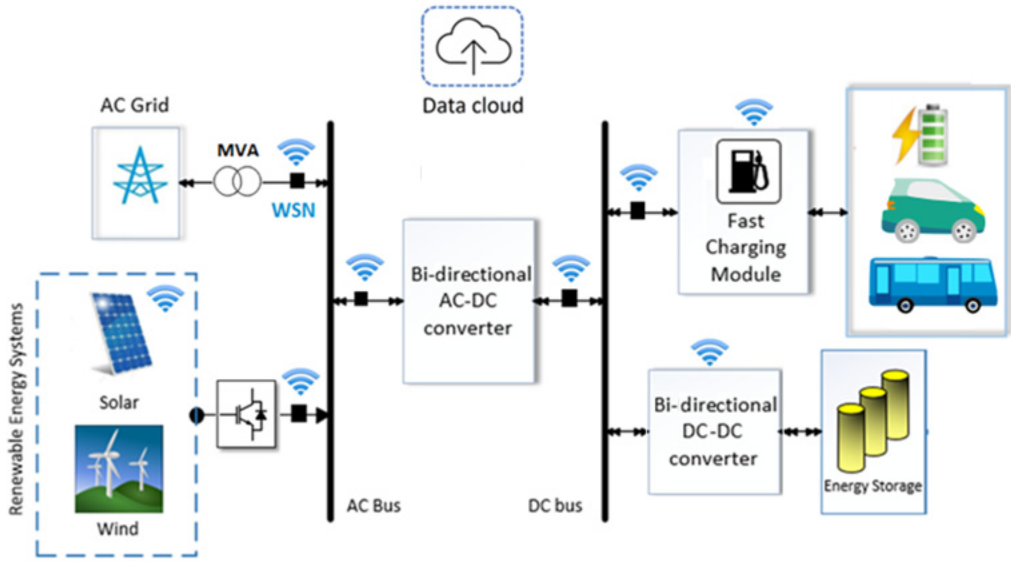

Figure 1. Mega power smart fast-charging station for electric vehicles.

3. Design Considerations

The proposed 1 MW charger section consists of three stages, as follows: an input filter to reduce the input distortion from the source side, which is also helpful for power factor improvement; an AC/DC converter; and three interleaved isolated DC/DC converters (each module of nearly 350 kW) that transform the required power to the battery. As discussed earlier, due to the high breakdown strength of UWBG devices, high bus voltage can be designed. In the designed infrastructure, one MVA capacity transformer steps down the high voltages to low voltages of 1400 V AC bus. The AC/DC PWM converter converts the AC voltage to regulated DC voltages of levels up to 3 kV DC. The charging station offers two modes of charging: mode 1 for electric vehicles with battery voltages up to 800–1000 V and mode 2 for heavy electric vehicles truck of voltages 1400–1600 V. Figure 2 represents the detailed schematic arrangement of the proposed charger.

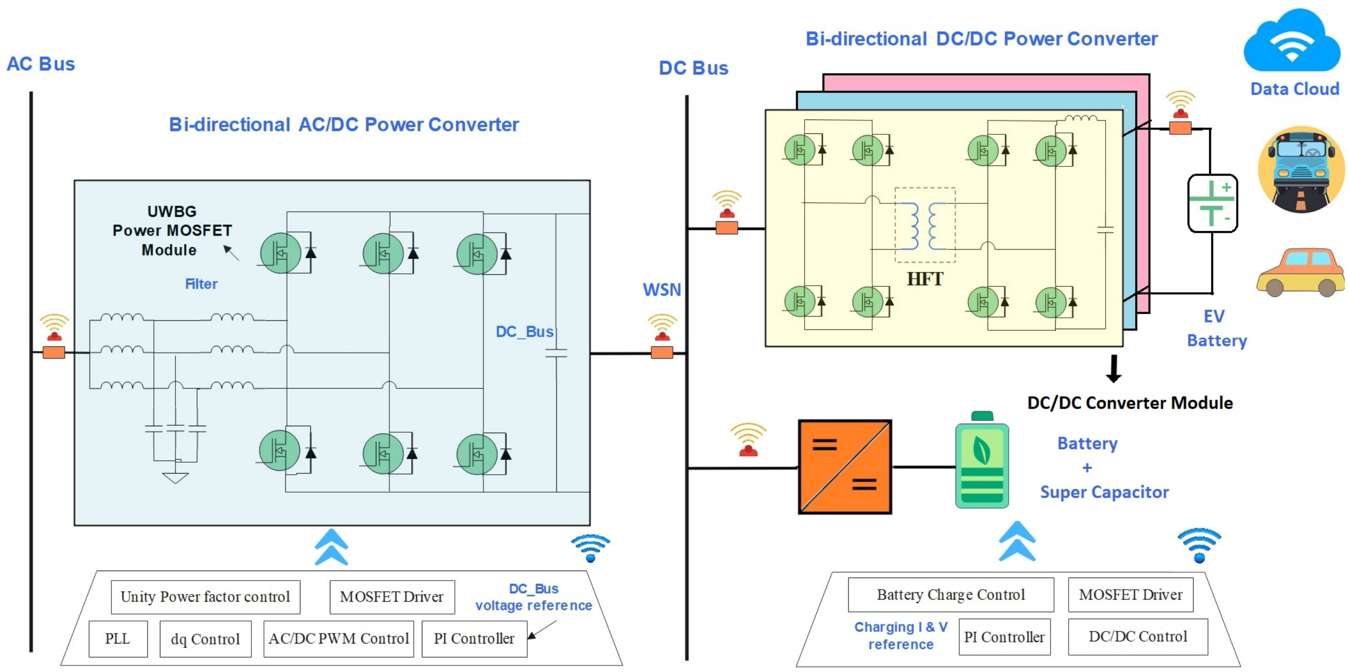

Figure 2. Schematic diagram of the smart EV charger using UWBG bidirectional power converters.

3.1. Stage 1: LCL Input Filter

The grid-connected AC/DC converter (PWM rectifier) operating at a typical switching frequency of order kHz causes harmonic distortion, which reduces the overall performance of the system. LCL filter provides the optimum results for power levels of hundreds of KVA with small filter values. To design a good LCL filter, certain criteria should be considered for optimum results. According to the design procedure mentioned in the paper [33,34], the following equations are used to find the optimum filter values (L_1, L_2, and C_{filter}) with a current attenuation of 30 A.

$$L_1 = \frac{V_{bus}\,(2 - m_a)}{4\,f_1\,\Delta i_{max}} \approx\ 1.0\,\mathrm{mH} \approx L_2 \tag{1}$$

$$C_{filter}(\max) = \frac{\lambda\,P_{grid}}{2\pi f_g\left(V_{grid}\sqrt{3}\right)^2} \approx\ 50\,\mu\mathrm{F} \tag{2}$$

where f_1, Δi_{max}, and m_a are the switching frequency, current attenuation, and modulation index of the AC/DC converter, respectively. The reactive power coefficient is denoted by λ, which has typical values in the range of 0.05 to 0.1. In the design, a capacitor value of 10 µF is selected. The resonance frequency (ω_{res}) generated by the LCL filter can be calculated using the following formula, which should satisfy the given condition [35].

$$\omega_{res} = \sqrt{\frac{L_1 + L_2}{L_1 L_2 C_{filter}}} \tag{3}$$

$$10\omega_g \leq \omega_{res} \leq \frac{1}{2}\omega_{sw1} \tag{4}$$

3.2. Stage 2: AC/DC Power Converter

A bidirectional AC/DC power converter is designed using a UWBG power module. PWM AC/DC converter can regulate the output DC voltage with a unity power factor control mechanism. The dq coordinate system with Clarks and Park's transform techniques is used for unity power control of the AC/DC power converter [36]. The wireless signal-based smart control system is designed using different controller and driver circuits. The grid voltages can be computed from the following equation, ignoring resistance.

$$V_{grid}(t) = L\frac{d}{dt}i_{grid}(t) + V_{AC/DC\_conv} \tag{5}$$

The converter's three-phase voltage and peak current equations in terms of MOSFET gate signals are evaluated below (neglecting the filter capacitor) [37].

$$V_a(t) = L\frac{d}{dt}i_a(t) + V_{DC}\left[S_a - \frac{1}{3}(S_a + S_b + S_c)\right] \tag{6}$$

$$V_b(t) = L\frac{d}{dt}i_b(t) + V_{DC}\left[S_b - \frac{1}{3}(S_a + S_b + S_c)\right] \tag{7}$$

$$V_c(t) = L\frac{d}{dt}i_c(t) + V_{DC}\left[S_c - \frac{1}{3}(S_a + S_b + S_c)\right] \tag{8}$$

$$I_{Peak} = I_{cnv1} = S_{11}I_a + S_{21}I_b + S_{31}I_c \tag{9}$$

where the terms 'a', 'b', and 'c' show each phase connected to the three legs of the converter. The total inductance is represented with the letter 'L'. The AC/DC converter's leg is controlled by two powers MOSFETs (power module). The control signal S_a (s11/s12), S_b (s21/s22), and S_c (s31/s32) are used to control the power flow of the converter.

To achieve a unity power factor at the grid side with independent control of both reactive and active current, the dq synchronous rotating coordinate system is used. In a rotating reference frame, the three-phase grid quantities are the first converted into an orthogonal stationary reference frame component system (alpha and beta) known as the Clarke transform. Then the system is converted into DC by projecting the stationary reference frame components (alpha and beta) on the rotating reference frame (dq). This transformation is known as the Parks transformation. The mathematical formulation to compare grid voltages with AC/DC converter voltages in the dq frame is given below [37]:

$$V_{AC/DC_{(d)}} = L\frac{di_{grid\_d}}{dt} - \omega L i_{grid\_q} + V_{grid\_d} \tag{10}$$

$$V_{AC/DC_{(q)}} = L\frac{di_{grid\_q}}{dt} + \omega L i_{grid\_d} + V_{grid\_q} \tag{11}$$

where $i_{grid(d,q)}$, $V_{grid(d,q)}$ are grid current and voltages in dq frame and $V_{DC/DC_{(d,q)}}$ are AC/DC converter voltages. To obtain a unity power factor, the reference value of the reactive component is set to zero (igrid_q = 0) and the AC/DC converter starts operating in a unity power factor.

3.3. Stage 3: DC/DC Power Converter

The DC/DC converter is designed using full-bridge topology (dual active bridge). A fully controlled power switch on both the primary and secondary sides makes it a bidirectional power converter. A high-frequency transformer (HFT) provides galvanic isolation between the charger and EV battery. The switching frequency of 50 kHz (f_2) is selected for the bidirectional DC/DC converter. Three interleaved modules of nearly 350 kW each are used to share the bulk charging current. The expression for output power of DC/DC converter including HFT efficiency factor η_t can be defined as follows [38]:

$$P_o = \eta_t V_o I_o = \left[\left\{\left(V_{bus} - 2V_{drp}\right)\frac{N_1}{N_2} - 2V_{drs}\right\}\frac{2T_{on}}{T_2} \times \left(S_{11}I_a + S_{21}I_b + S_{31}I_c\right)\right] \cdot \eta_t \tag{12}$$

where V_{drp} and V_{drs} represent the voltage drop of power devices at the primary and secondary sides of HFT. N_1 and N_2 are primary and secondary turn ratios of HFT (1:1).

3.4. High-Frequency Transformer Design Consideration

HFT is designed to handle more volts safely and accurately, converting high voltage and current levels between coils by magnetic induction. Each DC/DC converter module uses a separate HFT; to increase the core cross-section area, two identical cores are stacked together for the 350 kW HFT construction. A litz wire with 4000 strands is selected [39]. The following equations are used to select the core area product (A_p) and winding turns [40].

$$A_p = A_w A_c = \left(\frac{P_{max}}{K_1 \times B \times f_2}\right)^{\frac{4}{3}} = 6053 \text{ cm}^4 \tag{13}$$

$$N_1 = \frac{V \times 10^4}{K \times f_2 \times B \times A_c} \approx 17 = N_2 \tag{14}$$

where K_1 (0.017) and K (4) are topology and wave constant, respectively. 'B' represents the flux density whose value is typically 0.2 T. UU core (UF 240/480/60) is selected for winding with an area product of 7776 cm^4 and core area of A_c = 36 cm^2. The parameters are summarized in Table 2.

Table 2. Designed parameters for high-frequency transformer.

Parameter	Specification
Maximum power (P_{max})	350 KW each
High-frequency transformer (HFT) core	UF 240/480/60 × 2
Maximum magnetic flux density (B_{max})	0.2 T (tesla)
Bus voltages (V)	2500 V max.
Topology constant (K_1)	0.017
Wave constant (K)	4
High-frequency transformer (HFT) turns	17
Transformer area product (A_p)	7776 cm^4
Core area (A_c)	36 cm^2

3.5. Output Filter Values

The pulsating output voltage of the DC/DC converter is filtered for smooth charging operation of the EV battery. Assume that the ripple values of current (ΔI) and voltage (ΔV) are approximately 20 A and 40 V, respectively. The filter values can be calculated as [41]

$$L_o = \frac{V_{bus}\, D(1-D)}{f_2\, \Delta I} \approx 0.3 \text{ mH} \tag{15}$$

$$C_o = \frac{V_{bus}\, D(1-D)}{8 L_o F_2^2\, \Delta V} \approx 1 \text{ µF} \tag{16}$$

3.6. Design Summary

The grid-tied three-phase EV fast charger parameters are evaluated in this section for its design evaluation. The charger must provide the required current and voltage rating for charging the EV and HEV battery. The designed parameter of the proposed charger is summarized in Table 3.

Table 3. Proposed electric vehicle fast charger designed parameters.

Parameter	Specification
Rated charger power $\left(P_{grid}\right)$	1 MW (≈3 × 350 kW)
Input rated voltages AC bus $\left(V_{grid}\right)$	1400 V rms, 50 Hz
DC bus voltages ($\mathbf{V_{DC}}$)	2500 V max
Charging mode 1 (EV)	1200 V/800 A
Charging mode 2 (HEV)	2000 V/500 A
Switching frequencies for AC/DC and DC/DC converters ($\mathbf{f_1}, \mathbf{f_2}$)	20 kHz, 50 kHz
Average current across each MOSFET (AC/DC converters)	146 A
Average current across each MOSFET (DC/DC converters)	133 A
Input filter values ($\mathbf{L_1}, \mathbf{L_2}, \mathbf{C_f}$)	$L_{1,2}$= 10 mH C_f = 10 µF
Output filter ($\mathbf{L_o}, \mathbf{C_o}$)	0.3 mH, 1 µF

4. Simscape System Model

MATLAB Simscape is a powerful and flexible physical modeling tool for engineering system design. The MATLAB physical modeling systems consist of real physical components that can be modeled and simulated using actual realistic parameters [42,43]. The detailed and extensive simulation model of a proposed mega power smart EV charger is designed on the Simscape physical modeling tool (MATLAB) as per Table 3. The complete EV charger model contains many blocks and subsystems as shown in Figure 3.

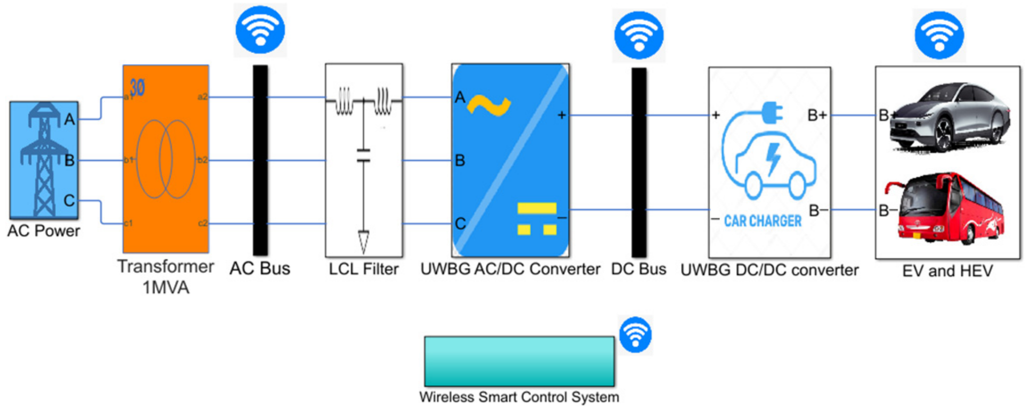

Figure 3. MATLAB model of smart mega power charging station.

MATLAB Simscape modeling supports SPICE model parameters including geometry variables. SPICE-compatible N-channel MOSFET blocks are used to model Ga_2O_3-based power devices using the SPICE parameter mentioned in the paper [27]. Virtual WSN sensors are used to collect data, and monitor and control the charging station. The smart system detects the battery parameters to select the appropriate mode of charging (EV-Mode 1 or HEV-Mode 2).

5. Simulation Analysis and Results

In the simulation analysis, both charging modes are studied and the behavior of grid response is observed. The model is created as per the mathematical models' equation mentioned in Section 3. The 11 kV grid voltage is stepped down to 1.4 kV (AC bus) by using a 1 MVA transformer. AC/DC converter generates the DC voltages as per the reference voltage set by the controller.

Mode 1 (EV mode) is designed for electric vehicles with a battery voltage range of up to 1200 V, which is suitable for the latest Tesla Founder series or future EVs. In this mode, the smart controller adjusts the DC bus voltages of up to 1800 V using an AC–DC converter. The DC–DC converter further controls the power levels according to the battery specifications. Mode 2 (HEV mode) is activated for charging heavy electric vehicles (electric buses, trucks, etc.) with a voltage range of up to 2000 V. The DC bus voltage is shifted to 2500 V using the control scheme of the AC–DC controller. The one-megawatt (I MW) power is transferred from the main grid to the designed fast charger at full capacity. The grid transient, steady-state, and transition (between HEV and EV modes) behavior are helpful for the analysis of the peak current characteristics and stable response time of the designed charger as shown in Figure 4c. Three-phase voltages and the current response of the AC bus while charging in both modes are shown in Figure 4.

In both charging modes, the active power delivered from the AC bus is nearly 1 MW. The simulation results validate the design procedure and smart control system of the proposed charger. The grid current and voltage response show the effectiveness of the design criteria of the LCL filter. The nearly sinusoidal behavior of grid current ensures the negligible current harmonics at the grid side. The stable grid response for the charging of EVs for both modes determines the satisfactory operation of charging infrastructure. The unity power factor control successfully transfers the active power of 1 MW from the grid to the charging converter without disturbing the phase angle between current and voltage. The power factor of 0.99 is achieved using the unity power factor method and the phase response of AC bus voltages and current are shown in Figure 5.

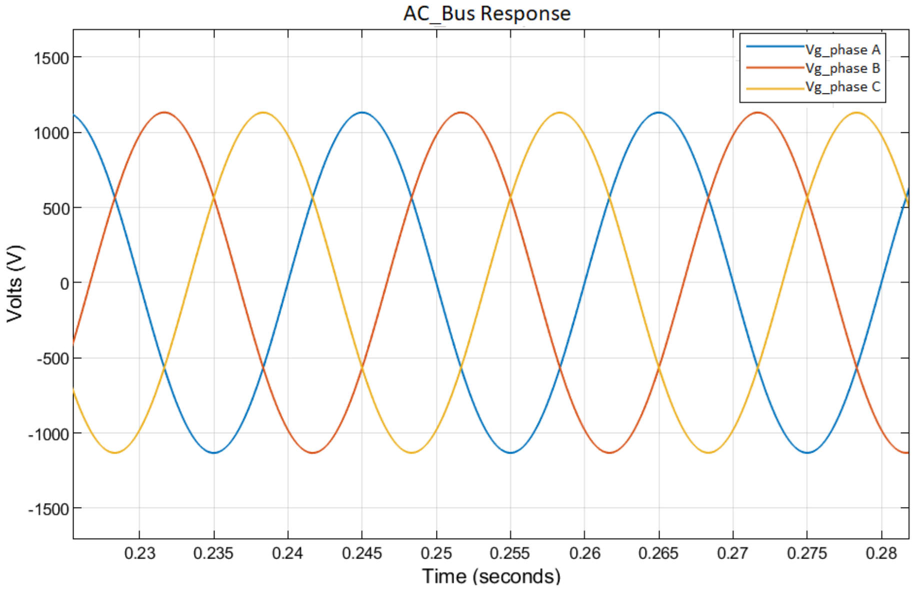

(**a**)

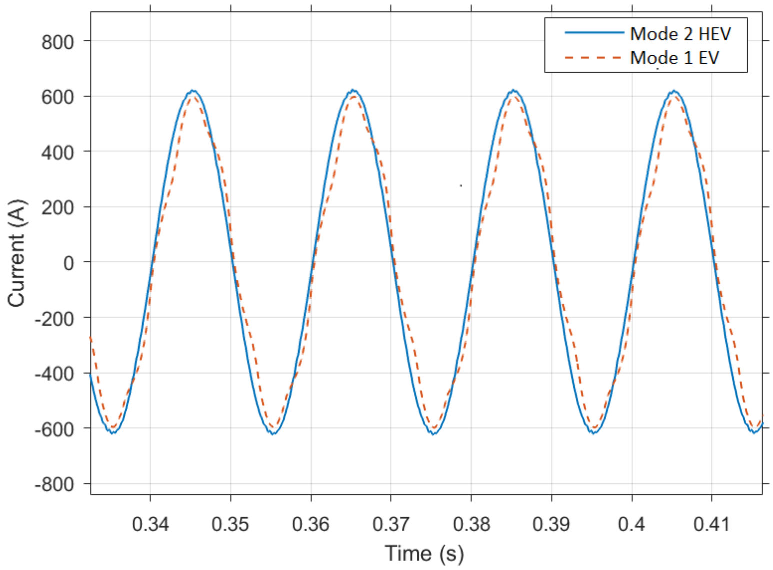

(**b**)

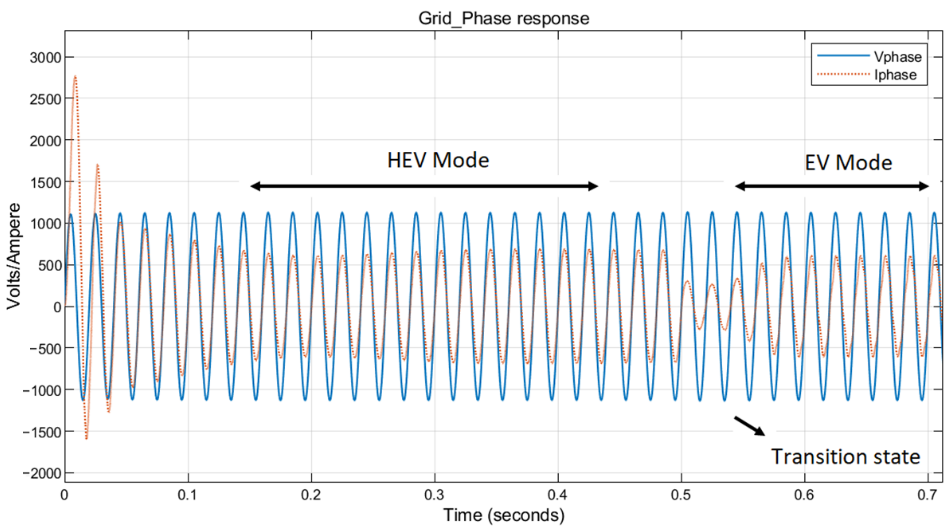

(**c**)

Figure 4. Three-phase response of AC bus (**a**) grid voltage response, (**b**) grid current behavior, (**c**) grid V−I phase response during HEV and EV charging.

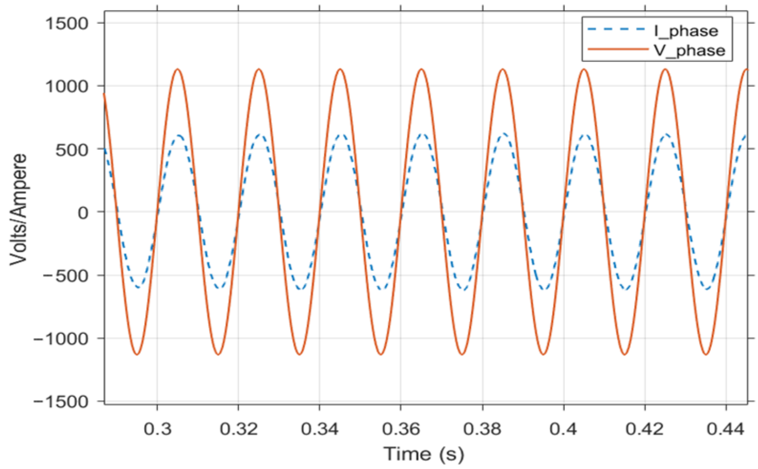

Figure 5. Unity power factor—controlled phase voltage and current response.

In both modes, DC bus voltages are regulated smartly using a control system by varying gate signals of the UWBG AC/DC power converter. For EV and HEV mode, DC bus voltages of 1800 V and 2500 V are set by smart controller, respectively. Figure 6 presents the DC bus behavior of the mega power charging system. The DC bus voltage is stable within 0.2 seconds of charging electric vehicles and only takes 0.1 seconds to shift from HEV mode to EV mode of charging as shown in Figure 6b.

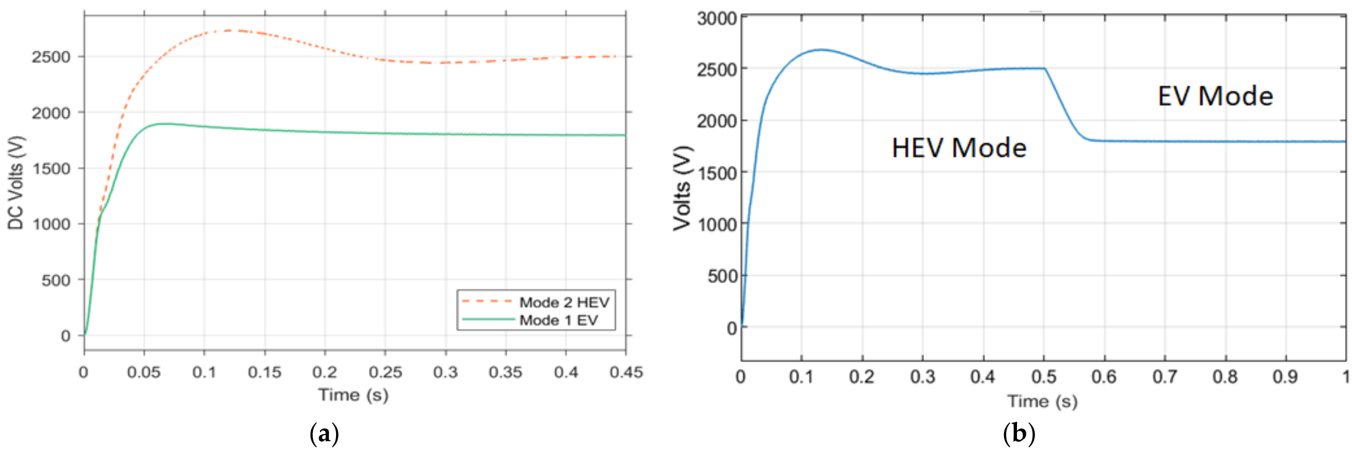

Figure 6. DC bus voltage response (**a**) HEV and EV charging modes, (**b**) DC bus response during transition state.

The DC/DC power controller works as a charge management system. The smart controller starts charging EV/HEV batteries effectively within 0.1 s. The charging voltage and current behavior of the DC/DC converter in both modes are presented in Figure 7.

The result shows that the proposed ultra-fast mega power EV charging station is the next-level infrastructure that will power both current and future electric vehicle battery technology. The charger is able to charge EV batteries up to a 2 kV voltage level with a power capacity of 1 MW due to the high voltage and current ratings of ultra-wide bandgap devices. The designed charger provides a wide range of charging levels for electric vehicles like the Tesla series and those designed by BMW, Nissan, Ford, etc. Due to the high voltage level, the charging time of EVs can be improved. The comparison of the proposed model with other DC fast chargers is summarized in Table 4.

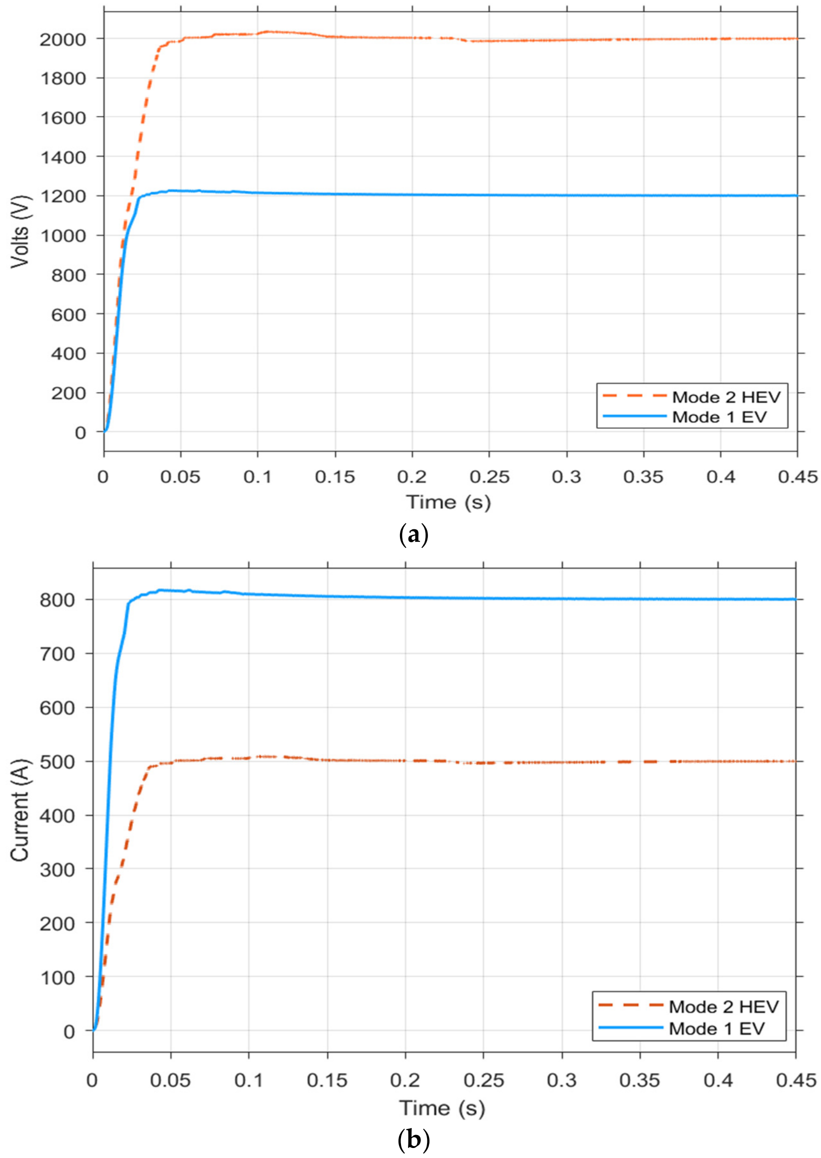

Figure 7. Charging response of EV and HEV (**a**) charging voltage, (**b**) charging current.

Table 4. Specification comparison of DC fast chargers [22,44].

Manufacturer	DC Voltage Range (V)	Max. Current (A)	Power (kW)
EVbox Tronics 100	≈50–500	200	100
EVTEC espresso and charge	≈170–500	300	150
Tesla Supercharger V3	≈880–970	640	250
ABB Terra HP GEN III	≈150–920	500	350
Tritium PK350	≈200–920	500	350
Proposed	≈360–2000	800	1000

6. Discussion

In this research, an electric vehicle charger design by using AC–DC and DC–DC power converter based on advanced power devices is discussed. The article highlights the important aspects of developing a reliable and efficient electric vehicle charging system for both electric vehicles and heavy-duty EVs. A three-phase AC/DC converter is connected to the power grid system using an LCL filter to reduce harmonics and improve power factor.

The detailed design procedure to find optimum LCL filter values for required power is analyzed with mathematical equations.

The mathematical model of an AC/DC power converter with unity power factor control is explained with detailed model equations. Three-phase voltage and current equations in terms of MOSFET gate signals are evaluated. The output voltage equation of the DC/DC converter is present considering MOSFET voltage drop and high-frequency transformer efficiency. The complete schematic arrangement with power, control, and gate driver signal is presented for a detailed understanding of the proposed scheme. Finally, the designed parameters are summarized for performance analysis. The extracted results validate the design procedure of the LCL input filter, output filter, mathematical equations of the converter, and model design parameters.

The proposed smart level 4 fast charger will be able to charge upcoming EV batteries of voltage levels up to 2 kV (capacity larger than 200 kWh). A wide range of power control reduces the complexity of using different chargers. High-power capacity EV chargers are the solution for upcoming electric vehicles. The increasing demand for high-capacity electric vehicle chargers needs efficient and optimum advanced material technology. Other than Ga_2O_3, more material devices like aluminum gallium nitride (AlGaN), aluminum nitride (AIN), etc., can be studied and analyzed.

7. Conclusions

The research presented the detailed design procedure of next-generation material-based 1 MW capacity charging infrastructure. The high voltage and current handling ability of the proposed ultra-wide bandgap power devices increases the charging potential of DC fast charges. The designed high-voltage charger will be useful for next-generation battery levels greater than 800 to 2000 V. The design parameter analysis helps to select the appropriate LCL filter for unity power factor control. The grid transient, steady-state, and transition analysis are important factors for designing protection schemes. The power converters parameter is preliminary useful for choosing appropriate power devices and sizing the high-frequency transformer for the selected switching frequency. The grid and charging response results illustrate the smooth stable behavior of the designed system for both types of charging modes, which validates the design procedure. The high charging current with a maximum voltage of 2000 V reduces the charging time of EVs and E-buses.

The complete mathematical modeling of the AC/DC/DC power converter is discussed. The research helps to develop a system that can charge upcoming high-capacity electric vehicle batteries with a voltage level greater than 800 V within a few minutes. The smart IoT control system increases system reliability and is helpful for service providers and customers in a wide range of applications. The proposed DC fast charger will easily charge 400 V small electric vehicles to large electric trucks with a battery voltage of up to 2000 V. The simulation analysis is useful to study the steady-state response, system behavior, optimization of passive components, and current harmonics. The research also encourages the EV automobile industry to design high battery capacity vehicles that will provide greater mileage and reduce charging anxiety on long routes. The designed infrastructure provides opportunities to install fast charging stations on highways, which is imperative for mass commercialization.

Author Contributions: Design and conceptualization, T.I. (Tehseen Ilahi) and T.I. (Tahir Izhar); methodology, T.I. (Tehseen Ilahi), M.Z. and A.R.; mathematical analysis, T.I. (Tehseen Ilahi), E.M.K. and A.R.; model validation, T.I. (Tahir Izhar), E.M.K., A.R. and T.Z.; formal analysis, T.I. (Tahir Izhar), M.Z. and K.T.; investigation, T.I. (Tahir Izhar); writing—original draft preparation, T.I. (Tehseen Ilahi), M.Z., K.T. and T.Z.; writing—review and editing, T.I. (Tehseen Ilahi), A.R., K.T. and T.Z. All authors have read and agreed to the published version of the manuscript.

Funding: This research received no external funding.

Data Availability Statement: Data are contained within the article.

Acknowledgments: The authors are grateful to the University of Engineering and Technology UET, Riphah International University, Lahore campus, and the University of Botswana for technical support.

Conflicts of Interest: The authors declare no conflicts of interest.

References

1. Leroutier, M.; Quirion, P. Air Pollution and CO_2 from Daily Mobility: Who Emits and Why? Evidence from Paris. *Energy Econ.* **2022**, *109*, 105941. [CrossRef]
2. Ilahi, T.; Zahid, T.; Zahid, M.; Iqbal, M.; Sindhila, A.; Tahir, Q. Design Parameter and Simulation Analysis of Electric Bike Using Bi-Directional Power Converter. In Proceedings of the 2020 International Conference on Electrical, Communication, and Computer Engineering (ICECCE), Istanbul, Turkey, 12–13 June 2020; pp. 1–6.
3. Town, G.; Taghizadeh, S.; Deilami, S. Review of Fast Charging for Electrified Transport: Demand, Technology, Systems, and Planning. *Energies* **2022**, *15*, 1276. [CrossRef]
4. Hardman, S.; Jenn, A.; Tal, G.; Axsen, J.; Beard, G.; Daina, N.; Figenbaum, E.; Jakobsson, N.; Jochem, P.; Kinnear, N.; et al. A Review of Consumer Preferences of and Interactions with Electric Vehicle Charging Infrastructure. *Transp. Res. Part D Transp. Environ.* **2018**, *62*, 508–523. [CrossRef]
5. Gupta, V.; Konda, S.R.; Kumar, R.; Panigrahi, B.K. Multiaggregator Collaborative Electric Vehicle Charge Scheduling Under Variable Energy Purchase and EV Cancelation Events. *IEEE Trans. Ind. Inform.* **2018**, *14*, 2894–2902. [CrossRef]
6. Chakraborty, S.; Vu, H.N.; Hasan, M.M.; Tran, D.D.; El Baghdadi, M.; Hegazy, O. DC-DC Converter Topologies for Electric Vehicles, Plug-in Hybrid Electric Vehicles and Fast Charging Stations: State of the Art and Future Trends. *Energies* **2019**, *12*, 1569. [CrossRef]
7. Carley, S.; Siddiki, S.; Nicholson-Crotty, S. Evolution of Plug-in Electric Vehicle Demand: Assessing Consumer Perceptions and Intent to Purchase over Time. *Transp. Res. Part D Transp. Environ.* **2019**, *70*, 94–111. [CrossRef]
8. De Santis, M.; Silvestri, L.; Forcina, A. Promoting Electric Vehicle Demand in Europe: Design of Innovative Electricity Consumption Simulator and Subsidy Strategies Based on Well-to-Wheel Analysis. *Energy Convers. Manag.* **2022**, *270*, 116279. [CrossRef]
9. Krueger, H.; Cruden, A. Integration of Electric Vehicle User Charging Preferences into Vehicle-to-Grid Aggregator Controls. *Energy Rep.* **2020**, *6*, 86–95. [CrossRef]
10. Leijon, J.; Boström, C. Charging Electric Vehicles Today and in the Future. *World Electr. Veh. J.* **2022**, *13*, 139. [CrossRef]
11. Pearton, S.J.; Ren, F.; Tadjer, M.; Kim, J. Perspective: Ga2O3 for Ultra-High Power Rectifiers and MOSFETS. *J. Appl. Phys.* **2018**, *124*, 220901. [CrossRef]
12. Lee, I.; Kumar, A.; Zeng, K.; Singisetti, U.; Yao, X. Modeling and Power Loss Evaluation of Ultra Wide Band Gap Ga_2O_3 Device for High Power Applications. In Proceedings of the 2017 IEEE Energy Conversion Congress and Exposition (ECCE), Cincinnati, OH, USA, 1–5 October 2017; pp. 4377–4382. [CrossRef]
13. Su, W.; Eichi, H.; Zeng, W.; Chow, M.-Y. A Survey on the Electrification of Transportation in a Smart Grid Environment. *IEEE Trans. Ind. Inform.* **2012**, *8*, 1–10. [CrossRef]
14. Liang, X.; Srdic, S.; Won, J.; Aponte, E.; Booth, K.; Lukic, S. A 12.47 KV Medium Voltage Input 350 KW EV Fast Charger Using 10 KV SiC MOSFET. In Proceedings of the 2019 IEEE Applied Power Electronics Conference and Exposition (APEC), Anaheim, CA, USA, 17–21 March 2019; pp. 581–587. [CrossRef]
15. Accelerate Vehicle Electrification with the Smallest, Lightest Power Modules | Vicor | Automotive. Available online: https://www.vicorpower.com/resource-library/ebook/auto-ebook (accessed on 8 October 2023).
16. Savio Abraham, D.; Verma, R.; Kanagaraj, L.; Giri Thulasi Raman, S.R.; Rajamanickam, N.; Chokkalingam, B.; Marimuthu Sekar, K.; Mihet-Popa, L. Electric Vehicles Charging Stations' Architectures, Criteria, Power Converters, and Control Strategies in Microgrids. *Electronics* **2021**, *10*, 1895. [CrossRef]
17. Coban, H.H.; Lewicki, W.; Sendek-Matysiak, E.; Łosiewicz, Z.; Drożdż, W.; Miśkiewicz, R. Electric Vehicles and Vehicle–Grid Interaction in the Turkish Electricity System. *Energies* **2022**, *15*, 8218. [CrossRef]
18. Ismail, A.; Abdel-Majeed, M.S.; Metwly, M.Y.; Abdel-Khalik, A.S.; Hamad, M.S.; Ahmed, S.; Hamdan, E.; Elmalhy, N.A. Solid-State Transformer-Based DC Power Distribution Network for Shipboard Applications. *Appl. Sci.* **2022**, *12*, 2001. [CrossRef]
19. Cervero, D.; Fotopoulou, M.; Muñoz-Cruzado, J.; Rakopoulos, D.; Stergiopoulos, F.; Nikolopoulos, N.; Voutetakis, S.; Sanz, J.F. Solid State Transformers: A Critical Review of Projects with Relevant Prototypes and Demonstrators. *Electronics* **2023**, *12*, 931. [CrossRef]
20. Yan, X.; Esqueda, I.S.; Ma, J.; Tice, J.; Wang, H. High Breakdown Electric Field in β-Ga_2O_3/Graphene Vertical Barristor Heterostructure. *Appl. Phys. Lett.* **2018**, *112*, 032101. [CrossRef]
21. Urooj, S.; Alrowais, F.; Teekaraman, Y.; Manoharan, H.; Kuppusamy, R. IoT Based Electric Vehicle Application Using Boosting Algorithm for Smart Cities. *Energies* **2021**, *14*, 1072. [CrossRef]
22. Acharige, S.S.G.; Haque, M.E.; Arif, M.T.; Hosseinzadeh, N.; Hasan, K.N.; Oo, A.M.T. Review of Electric Vehicle Charging Technologies, Standards, Architectures, and Converter Configurations. *IEEE Access* **2023**, *11*, 41218–41255. [CrossRef]
23. Zhang, M.; Liu, Z.; Yang, L.; Yao, J.; Chen, J.; Zhang, J.; Wei, W.; Guo, Y.; Tang, W. β-Ga_2O_3-Based Power Devices: A Concise Review. *Crystals* **2022**, *12*, 406. [CrossRef]

24. Meraj, S.T.; Yahaya, N.Z.; Lipu, M.S.H.; Islam, J.; Haw, L.K.; Hasan, K.; Miah, M.S.; Ansari, S.; Hussain, A. A Hybrid Active Neutral Point Clamped Inverter Utilizing Si and Ga2O3 Semiconductors: Modelling and Performance Analysis. *Micromachines* **2021**, *12*, 1466. [CrossRef] [PubMed]
25. Razzak, T.; Xue, H.; Xia, Z.; Hwang, S.; Khan, A.; Lu, W.; Rajan, S. Ultra-Wide Band Gap Materials for High Frequency Applications. In Proceedings of the 2018 IEEE MTT-S International Microwave Workshop Series on Advanced Materials and Processes for RF and THz Applications (IMWS-AMP), Ann Arbor, MI, USA, 16–18 July 2018; pp. 17–19. [CrossRef]
26. Zhang, Y.; Palacios, T. (Ultra)Wide-Bandgap Vertical Power FinFETs. *IEEE Trans. Electron Devices* **2020**, *1*, 1–12. [CrossRef]
27. Ilahi, T.; Izhar, T.; Qaisar, S.M.; Shami, U.T.; Zahid, M.; Waqar, A.; Alzahrani, A. Design and Performance Analysis of Ultra-Wide Bandgap Power Devices-Based EV Fast Charger Using Bi-Directional Power Converters. *IEEE Access* **2023**, *11*, 25285–25297. [CrossRef]
28. Richardson, D.B. Electric Vehicles and the Electric Grid: A Review of Modeling Approaches, Impacts, and Renewable Energy Integration. *Renew. Sustain. Energy Rev.* **2013**, *19*, 247–254. [CrossRef]
29. Hossein Motlagh, N.; Mohammadrezaei, M.; Hunt, J.; Zakeri, B. Internet of Things (IoT) and the Energy Sector. *Energies* **2020**, *13*, 494. [CrossRef]
30. Kombo, O.H.; Kumaran, S.; Bovim, A. Design and Application of a Low-Cost, Low- Power, LoRa-GSM, IoT Enabled System for Monitoring of Groundwater Resources With Energy Harvesting Integration. *IEEE Access* **2021**, *9*, 128417–128433. [CrossRef]
31. Savari, G.F.; Krishnasamy, V.; Sathik, J.; Ali, Z.M.; Abdel Aleem, S.H.E. Internet of Things Based Real-Time Electric Vehicle Load Forecasting and Charging Station Recommendation. *ISA Trans.* **2020**, *97*, 431–447. [CrossRef]
32. Suresh Kumar, R.; Rajesh, P.K.; Joys Nancy, J.; Abirami, S.; Vishnu Murthy, K. IoT-Based Monitoring and Management of Electric Vehicle Charging Systems for DC Fast Charging Facility. In *Internet of Things for Industry 4.0: Design, Challenges and Solutions*; Kanagachidambaresan, G.R., Anand, R., Balasubramanian, E., Mahima, V., Eds.; Springer International Publishing: Cham, Switzerland, 2020; pp. 147–159. ISBN 978-3-030-32530-5.
33. Majic, G.; Despalatovic, M.; Terzic, B. LCL Filter Design Method for Grid-Connected PWM-VSC. *J. Electr. Eng. Technol.* **2017**, *12*, 1945–1954. [CrossRef]
34. Liu, F.; Zhang, X.; Yu, C.; Shao, Z.; Zhao, W.; Ni, H. LCL-Filter Design for Grid-Connected Three-Phase PWM Converter Based on Maximum Current Ripple. In Proceedings of the 2013 IEEE ECCE Asia Downunder, Melbourne, VIC, Australia, 3–6 June 2013; pp. 631–635. [CrossRef]
35. Liserre, M.; Blaabjerg, F.; Hansen, S. Design and Control of an LCL-Filter-Based Three-Phase Active Rectifier. *IEEE Trans. Ind. Appl.* **2005**, *41*, 1281–1291. [CrossRef]
36. Frisfelds, K.; Krievs, O. Design of a Three-Phase Bidirectional PWM Rectifier with Simple Control Algorithm. *Latv. J. Phys. Tech. Sci.* **2019**, *56*, 3–12. [CrossRef]
37. Han, J.; Zhou, X.; Lu, S.; Zhao, P. A Three-Phase Bidirectional Grid-Connected AC/DC Converter for V2G Applications. *J. Control Sci. Eng.* **2020**, *2020*, 8844073. [CrossRef]
38. Pressman, A.; Billings, K.; Morey, T. *3-Half-Bridge and Full-Bridge Topologies, Switching Power Supply Design*, 3rd ed.; Mcgraw-hill: New York, NY, USA, 2009; pp. 111–115. ISBN 9780071482721.
39. Guo, Z.; Yu, R.; Xu, W.; Feng, X.; Huang, A.Q. Design and Optimization of a 200-KW Medium-Frequency Transformer for Medium-Voltage SiC PV Inverters. *IEEE Trans. Power Electron.* **2021**, *36*, 10548–10560. [CrossRef]
40. Rashid, M.H.; Rashid, H.M. *Magnetic Design Considerection, Power Supplies Chapter 13, Power Electronics: Circuits, Devices & Applications*, 4th ed.; Electrical and Computer Engineering; Taylor & Francis: Oxford, UK, 2017; ISBN 9780849334184.
41. Czarkowski, D. Converters. In *Power Electronics Handbook*, 4th ed.; Rashid, M.H., Ed.; Butterworth-Heinemann: Oxford, UK, 2018; pp. 275–288. ISBN 978-0-12-811407-0.
42. Tejado, I.; Torres, D.; Pérez, E.; Vinagre, B.M. Physical Modeling Based Simulators to Support Teaching in Automatic Control: The Rotatory Pendulum. *IFAC-PapersOnLine* **2016**, *49*, 75–80. [CrossRef]
43. Xu, B.; Lu, L.; Gong, D. Research on Real-Time Simulation of Power Electronic Circuits Based on Simscape. *J. Phys. Conf. Ser.* **2022**, *2196*, 012025. [CrossRef]
44. Srdic, S.; Lukic, S. Toward Extreme Fast Charging: Challenges and Opportunities in Directly Connecting to Medium-Voltage Line. *IEEE Electrif. Mag.* **2019**, *7*, 22–31. [CrossRef]